Adsorption Kinetics and Equilibria of Carbon Dioxide, Ethylene, and Ethane on 4A(CECA) Zeolite

A. Romero-Pérez and G. Aguilar-Armenta*

Facultad de Ciencias Químicas, Benemérita Universidad Autónoma de Puebla, 14 Sur y Av. San Claudio, Ciudad Universitaria, 72570 Puebla, Pue., México

The adsorption kinetics and equilibria of pure carbon dioxide (CO_2), ethylene (C_2H_4), and ethane (C_2H_6) on 4A(CECA) commercial zeolite have been measured over the temperature range $T = (293.15$ to $353.15)$ K using a glass-vacuum volumetric device. The adsorption rates of the gases were measured automatically via a custom acquisitions data card that was capable of registering pressure and time (t) data five times per second in the first period for $t = (0$ to $180)$ s, simultaneously. All of the gases showed a decreasing adsorption affinity and isosteric heat of adsorption in the order $CO_2 > C_2H_4 > C_2H_6$. Unlike CO_2, an activated diffusion for C_2H_4 and C_2H_6 for low t was observed. The adsorption activation energy for ethane $E_a = (14.6 \pm 0.2)$ kJ·mol^{-1} was found to be slightly higher than that for ethylene $E_a = (13.8 \pm 1)$ kJ·mol^{-1}. The dual Langmuir model described the CO_2 adsorption isotherms, whereas those for C_2H_4 and C_2H_6 were fitted with the Sips equation at (293.15 and 323.15) K. The three gases were reversibly adsorbed, and the adsorption selectivity for gas binary mixtures decreased in the sequence $CO_2/C_2H_6 > C_2H_4/C_2H_6 > CO_2/C_2H_4$. The obtained results indicate that 4A(CECA) zeolite could be a good candidate for separating these binary gas mixtures at 293.15 K.

Introduction

The separation of light hydrocarbon mixtures with very low relative volatilities as propylene/propane (1.1) and ethylene/ethane (1.5) using cryogenic distillation is a very expensive process. Nowadays, some energy-efficient alternative separation methods based on adsorption, absorption, membrane separation, and others have been developed. The adsorbent selectivity toward the olefin depends on a difference in either adsorption kinetics or adsorption equilibrium, as well as being determined by the ability of the adsorbent to exclude the larger molecule from the micropores.[1] Adsorbents for the separation of olefins from paraffins often include high surface area porous materials, which have been treated with transition metal species capable of π-complexation with olefins. Crystalline microporous adsorbents such as synthetic zeolites have attained great importance for gas separation. Adsorbents prepared by dispersing $AgNO_3$ over γ-Al_2O_3, SiO_2, and MCM-41 substrates are good candidates for ethane/ethylene and propane/propylene separations using pressure swing adsorption (PSA) processes.[2] It was found[3] that the 10Cu-MCM-48 adsorbent had a high adsorption capacity and selectivity toward ethylene and that all adsorption isotherms of C_2H_4 and C_2H_6 can be well-described by the Freundlich equation. Al-Baghli and Loughlin[4] studied the adsorption behavior of pure methane, ethane, and ethylene on an experimental titanium silicate (ETS-10). The adsorption data were analyzed using the Toth, unilan, and virial isotherms. These authors[5] also reported binary and ternary equilibrium adsorption data of methane, ethane, and ethylene on ETS-10 at (280.15 and 325.15) K and at pressures of (350 and 700) kPa. It was found that the separation of methane from ethane or ethylene is possible under any conditions. The following order of the adsorption uptakes $CH_4 < CO_2 < C_2H_4 \leq C_2H_6$ was reported[6] on silicalite-I over the temperature range $T = (305.15$ to $453.15)$ K. The isosteric heat of adsorption for these gases on silicalite-I lies between (18 and 32) kJ·mol^{-1}, with ethane having the highest value. The heat of sorption is affected slightly by the surface coverage for all of the gases, except for methane that decreases with increasing coverage.[6] The preference of the ZSM-5 zeolite for polar molecules such as carbon dioxide and ethylene increases as the Si/Al ratio decreases.[7] These authors observed a change in the relative adsorption capacity with the Si/Al ratio, the loading of CO_2 and C_2H_4 being increased, whereas the loading of C_3H_6 remains nearly constant for lower Si/Al ratios. Ethylene and ethane adsorption isotherms were measured for Engelhard ETS-10 exchanged with different mono-, di-, and trivalent cations.[8] Isotherms for Na-, K-, and Ag-ETS-10 were found to be nearly rectangular, indicating very strong adsorption. Breakthrough experiments demonstrate[9] that CuCl/NaX can be used as an effective adsorbent for the separation of ethylene and ethane mixtures. A maximum separation factor of 1.4 for ethylene over ethane is obtained[10] on a CuCl-modified γ-alumina membrane at $T = 333.15$ K. The interaction of ethylene and ethane with a Cu-tricarboxylate complex was investigated,[11] and a selective adsorption of ethylene by a factor of about 2 at low pressure was observed. The adsorption isotherms of methane, ethane, ethylene, and carbon dioxide[12] on ALPO-5 and SAPO-5 over the temperature range $T = (305$ to $353)$ K and pressure range $P = (0$ to $200)$ kPa were described by the Dubinin−Polanyi equation for all of the gases in both sorbents except for carbon dioxide in ALPO-5, which was described by the Freundlich model. The isosteric heat of adsorption of these sorbates and its variation with surface coverage differs widely for both sorbents.[12]

The main objective of this paper is to study the adsorption kinetics and equilibria of pure carbon dioxide (CO_2), ethylene (C_2H_4), and ethane (C_2H_6) on a 4A(CECA) commercial zeolite

* Corresponding author. E-mail address: geaguila0@gmail.com.

10.1021/je100215c
Published on Web 08/25/2010

sample, which was provided and manufactured by the CECA Co., Ltd. The adsorption kinetics and adsorption equilibrium isotherms have been measured over the temperature range $T =$ (293.15 to 353.15) K at subatmospheric pressures, using a glass volumetric system. The equilibrium adsorption data have been fitted to different adsorption isotherm equations. On the basis of the differences in the adsorption behavior of pure gases we propose the viability of using this sample for separating CO_2/C_2H_6, C_2H_4/C_2H_6, and CO_2/C_2H_4 mixtures. The extent of irreversible adsorption was also assessed.

Experimental Section

The adsorption ability of the 4A(CECA) zeolite sample to adsorb CO_2, C_2H_4, and C_2H_6 was measured in a homemade conventional glass high-vacuum volumetric device, equipped with grease-free valves and exhaustively calibrated with He. Pressures were registered with two types of pressure transducers (Balzers) of different ranges: TPR 017 [(0.0000133 to 0.399966) kPa] and APR 011 [(0.133322 to 101.3247) kPa]. The weight loss of the adsorbent was assessed by heating samples up to 623.15 K in a conventional oven under atmospheric pressure. Before the adsorption measurements, the samples were again heated in situ at 623.15 K in an oven until a residual pressure $P < 0.0001333$ kPa was reached and maintained at these conditions for 3 h. Subsequently, the temperature was decreased to the desired value and then the sample allowed to stabilize for at least 1.5 h before starting the measurements. A temperature in the interval $T =$ (293.15 to 373.15) K was controlled by a Haake L water ultrathermostat with a precision of $\pm$ 0.1 degree, and as for $T > 373.15$ K a programmable Lindberg oven with a control precision of $\pm$ 0.5 degree was used. The adsorbed amount was referenced to 1 g of the dehydrated adsorbent. The particles of the 4A(CECA) sample were spherical ($\sim$3 mm) pellets. The sample was previously characterized by means of a classical N_2 adsorption method at $T = 77.15$ K. As expected,[13] a very small N_2 adsorption uptake was detected. The obtained type-II N_2 adsorption isotherm, instead of the common type-I adsorption isotherms for zeolites, shows that at low temperature the rate of diffusion of N_2 molecules into the intracrystalline micropore structure is extremely slow, and consequently the adsorption equilibrium is not achieved in a reasonable time. The N_2 adsorption isotherm was described fairly well with the Brunauer−Emmett−Teller model over a relative vapor pressure range $P/P_o =$ (0.01 to 0.35) with an apparent external surface area $S = (10 \pm 1.5)$ $m^2 \cdot g^{-1}$. During the kinetic measurements the decrease of pressure in the system from $P_{in} = 59.9949$ kPa ($t = 0$) to equilibrium pressure (P_{eq}) was measured automatically with a custom acquisition data card which allowed simultaneous monitoring and recording of time and pressure data. In the period $t =$ (0 to 180) s the pressure was monitored five times per second. Afterward, in the period $t =$ (3 to 13) min, pressure was registered once per second, and in the period of 13 min to equilibrium, pressure was recorded once every 10 s. To verify the quality and reproducibility of the data, some measurements were repeated.

To evaluate the extent of irreversible adsorption, which is the adsorbed amount that cannot be removed under vacuum at a given experimental temperature, the experiments were performed as follows. To assess the total adsorption uptake at a given temperature an initial adsorption kinetic curve $[n_{Total} = f(t)]_T$ was measured. Afterward, the sample was subjected to a vacuum at the same temperature as in the prior experiment until a residual pressure of 1.333 Pa was reached, and then a second kinetic curve was measured $[n_{Rev} = f(t)]_T$. After the second measurement the sample was again degassed at the same experimental temperature, and then a third kinetic curve was measured. The irreversibly adsorbed amount was assessed by the difference in amount adsorbed between the first (total) and the second (reversible) kinetic adsorption curves. The measurements of the adsorption−desorption cycles were repeated up to three times in both adsorption kinetics and equilibria for all gases.

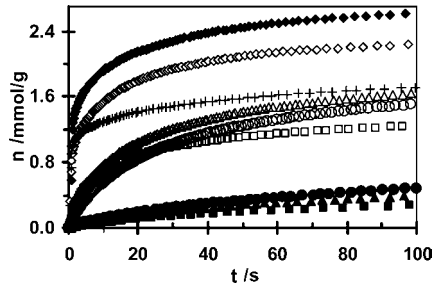

Figure 1. Gas adsorption uptake as a function of contact time t at different temperatures T/K: CO_2 (◆, 293.15; ◇, 323.15; +, 353.15), C_2H_4 (△, 293.15; ○, 323.15; □, 353.15), C_2H_6 (●, 293.15; ▲, 323.15; ■, 353.15).

Table 1. Polarizability, α, Quadrupole Moment, δ, and Critical Diameter, σ_{cr}, of Gases[13]

property	C_2H_6	C_2H_4	CO_2
α/Å^3	3.9	3.5	1.9
δ/Å^3	0.27	0.48	0.64
σ_{cr}/Å	3.72	3.44	3.1

Results and Discussion

Adsorption Kinetics. Figure 1 shows that both the adsorption rate and the adsorption capacity for $T =$ (293.15 to 353.15) K decrease in the same order of the decreasing quadrupole moment ($CO_2 > C_2H_4 > C_2H_6$) and increasing critical diameter ($CO_2 < C_2H_4 < C_2H_6$) of the gas molecules[13] (Table 1). A good coincidence among the first, second, and third adsorption kinetic curves for the three gases was observed. The absence of irreversible adsorption should facilitate to a great extent the regeneration of the adsorbent in gas separation cyclic processes as in the PSA cycles. The results showed that the adsorption uptake decreased and the initial rate of CO_2 adsorption did not change with increasing temperature since this molecule diffuses freely into micropores giving a very fast adsorption. On the contrary, an increase of the adsorption rate of C_2H_4 and C_2H_6 for low contact time t with increasing temperature was observed.

To examine with more detail the influence of temperature on the hydrocarbon adsorption rate, the variation of the fractional pore filling n_t/n_{eq} as a function of t was analyzed (Figure 2), where n_t and n_{eq} are the amounts adsorbed at a given time t and equilibrium, respectively. The obtained results revealed that the adsorption rate increases with increasing temperature, that is,

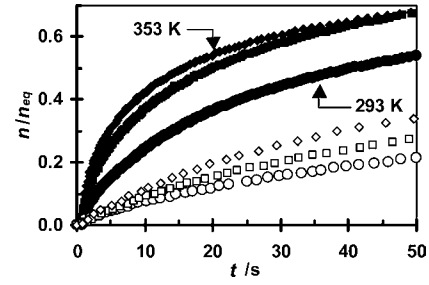

Figure 2. Fractional pore filling for C_2H_4 (closed symbols) and C_2H_6 (open symbols) as a function of t at different temperatures T/K): ●, ○, 293.15; ■, □, 323.15; ◆, ◇, 353.15.

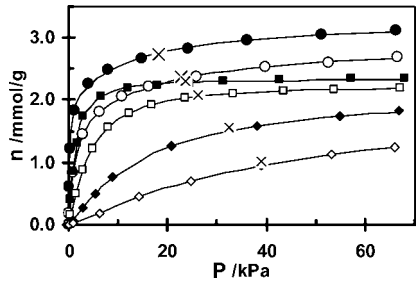

Figure 3. Adsorption isotherms at $T_1 = 293.15$ K (closed symbols) and $T_2 = 323.15$ K (open symbols): ●, ○, CO_2; ■, □, C_2H_4; ◆, ◇, C_2H_6. Kinetic adsorption data at equilibrium (×).

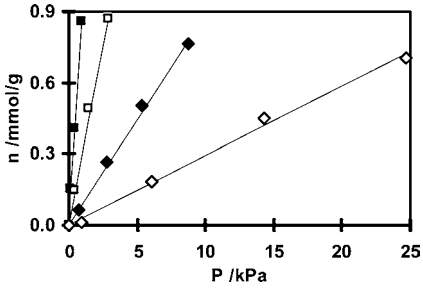

Figure 4. Henry adsorption isotherms at $T_1 = 293.15$ K (closed symbols) and $T_2 = 323.15$ K (open symbols): ■, □, C_2H_4; ◆, ◇, C_2H_6.

the activated diffusion of C_2H_4 and C_2H_6 molecules through zeolite channels is the rate-controlling process in the adsorption of these gases over the temperature range $T = (293.15$ to $353.15)$ K. The time $t_{1(0.5)}$/(s) and $t_{2(0.5)}$/(s) corresponding to one-half of the fractional uptake ($n_t/n_{eq} = 0.5$) at $T_1 = 293.15$ K and $T_2 = 353.15$ K, respectively, acquired the following values: for C_2H_4 (40.5, 15.6) and for C_2H_6 (309, 112). Equation 1 that was proposed by Timofeev and Erashko[14] was used to estimate the adsorption activation energy E_a of the gases. A similar E_a was found for both gases: $E_a(C_2H_4) = (13.8 \pm 1)$ kJ·mol^{-1}, $E_a(C_2H_6) = (14.6 \pm 0.2)$ kJ·mol^{-1}. This could be due to the small difference in their molecular size (Table 1). Interestingly, Dewitt et al.[15] have found slightly smaller activation energy values, $E_a = (12.5 \pm 2)$ kJ·mol^{-1} and $E_a = (11.5 \pm 3)$ kJ·mol^{-1}, on microporous silica for ethylene and ethane, respectively.

$$E_a = \frac{RT_1T_2}{T_1 - T_2} \ln \frac{t_{2(0.5)}}{t_{1(0.5)}} \quad (1)$$

Adsorption Equilibrium. Knowledge of single-gas adsorption equilibrium isotherm behavior is essential to design a specific adsorptive gas separation process. Figure 3 compares the adsorption isotherms of CO_2, C_2H_4, and C_2H_6 at $T_1 = 293.15$ K and $T_2 = 323.15$ K. Apparently, to achieve better results the equilibrium adsorptive separation process should be performed at $P < 5$ kPa. The gas-adsorbed amounts at equilibrium during the kinetic measurements (× points in Figure 3) at the respective operational temperature agree fairly well with the respective adsorption isotherms. In contrast with CO_2, the adsorption equilibrium isotherms for C_2H_4 and C_2H_6 at $P < 25$ kPa behaved according to the Henry law equation (Figure 4) with a coefficient of determination $R^2 = 0.999$.

The enthalpy of adsorption ($-\Delta H_0$), which was evaluated using the van't Hoff equation, eq 2, and the separation factor $\alpha = K_{H(C_2H_4)}/K_{H(C_2H_6)}$ as the ratio of Henry constants K_H, which decreases slightly with increasing temperature ($\alpha = 10.5$ for $T_1 = 293.15$ K and $\alpha = 10.0$ for $T_2 = 323.15$ K), are cited in Table 2. A similar separation factor value ($\alpha = 9.8$) was found using the empirical equation [$\log \alpha = 4.76(1 - \beta_2/\beta_1) - 0.23$], which was proposed by Keltsev[16] for the adsorption of gases on zeolites, where $\beta_{2(C_2H_6)} = 1.68$ and $\beta_{1(C_2H_4)} = 2.26$ are the affinity coefficients for the less and more adsorbed gas, respectively.

Table 2. Henry Constants, K_H, Pressure Range, Enthalpy of Adsorption, $-\Delta H_0$, Adsorption Net Heat, $Q_n = \Delta H_0 - \Delta H_{liq}$, and Separation Factor, α

	C_2H_4		C_2H_6		α	α
T/K	293.15	323.15	293.15	323.15	293.15	323.15
pressure range/kPa	0.01−0.9	0.4−2.9	0.75−8.8	0.9−24.7		
K_H/mmol·g^{-1}·kPa^{-1}	0.9451	0.300	0.0900	0.030	10.5	10
$-\Delta H_0$/kJ·mol^{-1}	30.1		28.8			
Q_n/kJ·mol^{-1}	16.6		14.1			

Table 3. σ, Standard Deviation Values Calculated for the CO_2, C_2H_4, and C_2H_6 Adsorption Isotherms[a]

gas	T/K	dual Langmuir	Sips	Toth	Langmuir
CO_2	293.15	0.02218	0.04187	0.06349	0.35506
	323.15	0.02096	0.02644	0.03190	0.12650
C_2H_4	293.15	0.07487	0.02015	0.03504	0.07684
	323.15	—	0.00962	0.01043	0.06177
C_2H_6	293.15	—	0.00852	0.01472	0.04852
	323.15	—	0.00470	0.02310	—

[a] The standard deviation σ is calculated as $\sigma = [\sum_i^j((n_{exp} - n_{calc})^2)/(j - m)]^{1/2}$ where n_{exp} are the experimental adsorbed amounts (mmol·g^{-1}), n_{calc} the predicted amounts by the respective adsorption isotherm equation (mmol·g^{-1}), j the number of data points, and m the number of fitted parameters.

$$-\Delta H_0 = R\left(\frac{T_1T_2}{T_1 - T_2}\right)\ln\left(\frac{K_2}{K_1}\right) \quad (2)$$

The classical Langmuir, dual Langmuir, Sips, and Toth equations were used to find which one best describes the equilibria data. Table 3 compares the standard deviation (σ) computed for the three gases. Although a good coefficient of determination $R^2 = 0.996$ of Langmuir plots (P/n vs P) for the CO_2 adsorption isotherms was obtained, a poor description of the adsorption equilibrium data was observed, mainly at low pressures, because one or various assumptions made in this ideal theory are not fulfilled. The Langmuir equation gave a better description of the C_2H_4 adsorption isotherms than those for CO_2. The data in Table 3 show that the dual Langmuir equation, eq 3, that implicitly takes into account interactions between adsorbed molecules and two (1 and 2) energetic adsorption sites, was found to be the best one to fit the CO_2 adsorption isotherms but did not describe those for C_2H_4 and C_2H_6. The Sips equation (eq 4) and Toth equation (eq 5) gave an excellent description of the C_2H_4 and C_2H_6 adsorption isotherms at $T_1 = 293.15$ K and $T_2 = 323.15$ K over the whole pressure range studied. The fitting of experimental data with these equations was done using a computational program written in Matlab,[17] and the obtained optimal parameters are given in the Table 4 for those adsorption equations that gave the best description.

$$n = n_{m1}\frac{K_1P}{1 + K_1P} + n_{m2}\frac{K_2P}{1 + K_2P} \quad (3)$$

Here n_{m1} and n_{m2} are the maximum adsorbed amount, and K_1 and K_2 are the adsorption equilibrium constants for the adsorption sites 1 and adsorption sites 2, respectively.

$$n = \frac{n_m (KP)^{1/N}}{1 + (KP)^{1/N}} \quad (4)$$

$$n = \frac{n_m KP}{[1 + (KP)^t]^{1/t}} \quad (5)$$

When $N = 1$ and $t = 1$, eqs 4 and 5 reduce to the classical Langmuir equation. This means that if N and t are different from unity it may be assumed that factors, such as adsorbate−adsorbate interactions, energetic heterogeneity, irreversible adsorption, or others, may be significant in a given adsorption process. It is evident that the more N deviates from unity, the more heterogeneous is the adsorbent−gas system.

The enthalpy of adsorption, $-\Delta H_a$ (Table 4), of gases was evaluated using the van't Hoff eq 2 and the equilibrium constants K. From the adsorption data it can be seen that the interaction of the adsorption sites 1 with CO_2 molecules is significantly stronger ($-\Delta H_a = 47.8$ kJ·mol^{-1}) than that of the adsorption sites 2 ($-\Delta H_a = 10.6$ kJ·mol^{-1}), which is even smaller than its latent heat of condensation (17.15 kJ·mol^{-1}). It was observed (Figure 5) that 99.1 % of CO_2 adsorbed molecules at $T_1 = 293.15$ K are located in the sites 1 at $P = 0.018$ kPa. Because the sites 2 are progressively filled with increasing pressure, coverage of 65 % corresponds to sites 1 at saturation. A similar behavior for the CO_2 adsorption isotherm at $T_2 = 323.15$ K was observed. As is well-known,[13,18,19] of the 12 Na^+-cations per ∝-cage in the dehydrated 4A zeolite, eight are located in the cation-type I sites, three in cation-type II sites, and one in cation-type III sites. This gives a cation relative distribution decrease (%) in the sequence: cation-type I (66.66) > cation-type II (25) > cation-type III (8.33).

On the basis of the relative contribution of the adsorption site 1 on the total adsorption capacity tends to a fractional uptake of 0.65 for the high-coverage region (Figure 5), it can be assumed that the CO_2 molecules adsorb preferentially on the Na^+-cations located near apertures in the cation-type I sites, where one molecule is adsorbed onto one Na^+-cation.

Adsorption Selectivity. Adsorption equilibrium behavior for CO_2/C_2H_6, C_2H_4/C_2H_6, and CO_2/C_2H_4 mixtures was assessed using pure component adsorption isotherm data and the ideal adsorbed solution theory.[20,21] Figure 6 depicts the variation of the adsorbed mole fraction X as a function of gas mole fraction Y at $T_1 = 293.15$ K. The adsorption selectivity α was assessed from the adsorption phase diagram using the relation $\alpha = X_1Y_2/X_2Y_1$, where X and Y are the equilibrium mole fractions in the adsorbed and gas phases, respectively. Subscripts 1 and 2 refer to more adsorbed and less adsorbed gas, respectively, for a given binary gas mixture. The results obtained at $T_2 = 323.15$ K were very similar to those recorded at T_1. As can be seen from Figure 6, all three equilibrium curves are situated above the diagonal, for which $\alpha = 1$. Evidently, the more marked is the deviation from the diagonal the better is the separation. Figure 7 shows very high adsorption selectivity for CO_2 (or C_2H_4) at low Y and decreases continuously with increasing Y.

Table 4. Fitting Parameters by Dual Langmuir (DL) and Sips Models, Enthalpy, $-\Delta H_a$, and Net Heat, Q_n, of Adsorption

	293.15 K	323.15 K	$-\Delta H_a$ / kJ·mol^{-1}	Q_n / kJ·mol^{-1}
CO_2	DL	DL		
n_{m1}/mmol·g^{-1}	2.0236	1.8044		
K_1/kPa	5.4550	0.8800	47.8	30.65
n_{m2}/mmol·g^{-1}	1.3033	1.1720		
K_2/kPa	0.0731	0.0488	10.6	−4.1
C_2H_4	Sips	Sips		
n_m/mmol·g^{-1}	2.3393	2.2579		
K/kPa	0.7418	0.2415	29.4	15.9
N	0.7791	0.8044		
C_2H_6	Sips	Sips		
n_m/mmol·g^{-1}	2.1469	1.8082		
K/kPa	0.0661	0.0282	24	9.3
N	0.88070	0.8107		

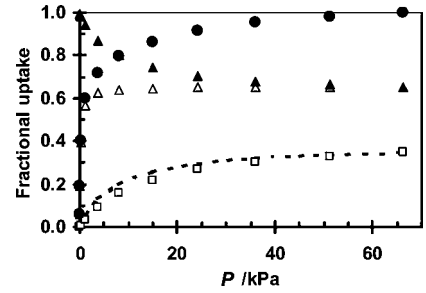

Figure 5. Total uptake (●) for CO_2. Fractional uptake for site 1 (△) and site 2 (□). Contribution of site 1 (▲) and site 2 (dotted line) at 293.15 K.

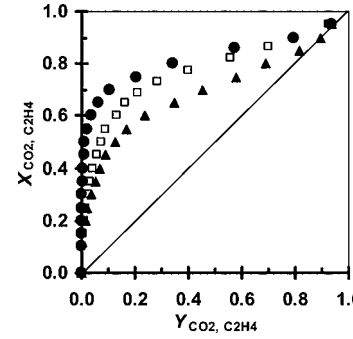

Figure 6. Adsorbed mole fraction X as a function of gas mole fraction Y at $T_1 = 293.15$ K. ●, CO_2/C_2H_6; □, C_2H_4/C_2H_6; ▲, CO_2/C_2H_4.

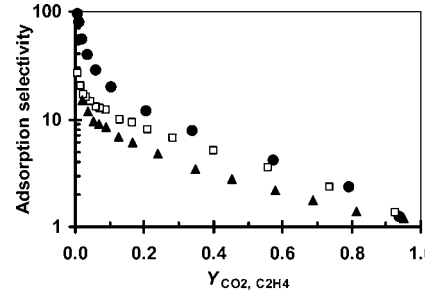

Figure 7. Adsorption selectivity as a function of gas mole fraction Y at $T_1 = 293.15$ K. ●, CO_2/C_2H_6; □, C_2H_4/C_2H_6; ▲, CO_2/C_2H_4.

The selectivity toward CO_2 and C_2H_4 shown by zeolite adsorbents depends on the predominant interaction energy, which is determined by the physical properties of gases, such as quadrupole moment, polarizability, and others. These results show that the equilibrium adsorption selectivity decreases in the same order of decreasing quadrupole moment difference $\delta_1 - \delta_2$ (Å^3) between the gases (Table 1), that is, CO_2/C_2H_6 (0.37) > C_2H_4/C_2H_6 (0.21) > CO_2/C_2H_4 (0.16).

The ratio of the adsorbed amount of pure gases (n_i/n_j) at different equilibrium pressures at $T_1 = 293.15$ K (Table 5) also decreases in this sequence, but there are differences in selectivity values, mainly at very low gas phase concentrations. It can be seen that the biggest difference is observed for the CO_2/C_2H_6 and CO_2/C_2H_4 mixtures. Unlike the adsorption of pure gases,

Table 5. Pure Gas Adsorption Selectivity Ratio at $T_1 = 293.15$ K

P/kPa	CO_2/C_2H_6	C_2H_4/C_2H_6	CO_2/C_2H_4
1	22.12	11.62	1.9
2	10.00	7.45	1.34
6	4.44	3.75	1.18
10	3.07	2.59	1.18
20	2.27	1.84	1.23
30	2.00	1.58	1.29

the competition for occupying the adsorption sites for mixture adsorption on polar surfaces is determined by the stronger interaction of that molecule that has the biggest quadrupole moment. The lowest selectivity in Table 5 for the CO_2/C_2H_4 mixture is possibly due to the exclusive olefin π-bond interaction. Owing to the high adsorption selectivity toward carbon dioxide and ethylene and on the reversible adsorption observed for all gases, which acquires a relevant importance for adsorbent regeneration, the 4A(CECA) zeolite could be a potential adsorbent for separating CO_2/C_2H_6, C_2H_4/C_2H_6, and CO_2/C_2H_4 mixtures at 293.15 K.

Comparing the C_2H_4 and C_2H_6 adsorption isotherms on 4A(CECA) zeolite (Figure 4) with those reported by Al-Baghli and Loughlin[5] on titanosilicate (ETS-10) zeolite at $T = 325.15$ K, a greater difference in adsorption uptake of gases on 4A(CECA) than ETS-10 zeolite can be seen. In addition, because the adsorption isotherms for both gases on ETS-10 are more rectangular than on 4A(CECA), the separation of ethylene from ethane should be more practical on this zeolite. The adsorption uptake of both ethane and ethylene on HMS-type mesoporous silica at $T = 303.15$ K varies almost linearly with pressure.[22] Although this is one of the important criteria for the choice of an adsorbent for adsorption separation, the authors found a small adsorption selectivity value $\alpha = 1.6$. The adsorption capacities for carbon dioxide, ethylene, and ethane on 13X zeolite[23] at 323 K are very similar to those on 4A(CECA). It seems that both samples would have similar separation efficiency.

Isosteric Heat of Adsorption. Because the adsorption is an exothermic process, the information of heat released is very important for separating gas mixtures. The isosteric heat of adsorption (Q_{st}) with gas loading was computed from the adsorption equilibrium isotherms (Figure 3) measured at $T_1 = 293.15$ K and $T_2 = 323.15$ K using the Clausius−Clapeyron equation, eq 6, for a given constant adsorbate loading (n).

$$\frac{Q_{st}}{RT^2} = -\left[\frac{\partial \ln P}{\partial T}\right]_n \tag{6}$$

To compare the strength of the bonding between adsorptive and surface, it is more helpful to subtract the nonspecific dispersion and repulsion contributions (heat of liquefaction) from the isosteric heat, that is, consider only the specific contributions: polarization, field−dipole, and field−gradient−quadrupole energies. The variation in net isosteric heat of adsorption with loading (Figure 8) decreased as follows: $CO_2 > C_2H_4 > C_2H_6$, which is in concordance with the decreasing order of the quadrupole moment of the gas molecules (Table 1). The enthalpy of adsorption (dotted lines in Figure 8) that was assessed by means of eq 2 (Table 4) was situated near the average of the adsorption heat profile.

As can be seen from Figure 8, the isosteric heat of adsorption is slightly higher for C_2H_4 than for C_2H_6 but for CO_2 was found to be considerably higher than that for C_2H_4. Because of the adsorption of nonpolar molecules, such as ethane, only non-

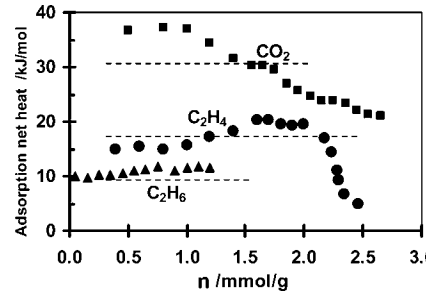

Figure 8. Adsorption net heat as a function of loading. Dotted lines are the adsorption heat by the van't Hoff equation.

specific interactions can contribute to adsorption energy, which are mainly determined by its polarizability; the contribution of the π-bond of ethylene ($-\Delta H_{\pi\text{-bond}}$) and the quadrupolar moment ($-\Delta H_\delta$) of CO_2 to the total adsorption energy may be assessed by the difference between the respective adsorption heat profiles: ($-\Delta H_{\pi\text{-bond}} = Q_{C_2H_4} - Q_{C_2H_6}$) and ($-\Delta H_\delta = Q_{CO_2} - Q_{C_2H_6}$). As expected, Figure 8 shows that $-\Delta H_\delta \gg -\Delta H_{\pi\text{-bond}}$.

Figure 8 also shows that, for the three gases, the adsorption heat profiles for low coverage remain more or less constant, which could be due to a compensating effect of the interaction between the adsorbed molecules and the surface heterogeneity. A tendency to increase for both hydrocarbons, principally for C_2H_4, is observed with loading, which could indicate that the intermolecular attraction forces dominate. For the strongly quadrupolar CO_2 molecule, the heat of adsorption remains more or less constant up to a loading of 0.9 mmol·g^{-1}, beyond which it decreases. Because of the nearly rectangular shape of the CO_2 adsorption isotherms and the absence of experimental data at very low pressures, the evaluation with acceptable accuracy of CO_2 adsorption isosteric heat for low coverage (< 0.5 mmol·g^{-1}) was particularly difficult. Afterward, a monotonic decrease with increasing coverage is observed, that is, the interactions between adsorption surface sites and adsorbate molecules (surface heterogeneity) dominate. Because the high contribution of the field gradient−quadrupole energy of CO_2 can lead to a temperature increase of adsorbent particle, it is essential to control the rate of particle cooling in the adsorption separation process.

As a result of the absence of any cation in silicalite-I and, consequently, the nonexistence of the polarizing effect, the authors[6] observed an opposite order of the heat of adsorption, $C_2H_6 > C_2H_4 > CO_2$, which is consistent with the gas molecular weight decrease. Compared with 4A(CECA), a similar adsorption heat value (28.4 kJ·mol^{-1}) for C_2H_6 has been reported[24] but a considerably higher value for C_2H_4 (44.5 kJ·mol^{-1}) on 4A zeolite pure crystals. Perhaps, the absence of binder in 4A zeolite was the reason of the stronger adsorption of ethylene on this sample.

Conclusions

The study of kinetic and equilibrium adsorption of carbon dioxide (CO_2), ethylene (C_2H_4), and ethane (C_2H_6) on 4A(CECA) zeolite showed that the gases were adsorbed reversibly and that the gas adsorption capacity decreased in the order $CO_2 > C_2H_4 > C_2H_6$. Unlike CO_2, the adsorption rate of C_2H_4 and C_2H_6 for low t increases with increasing temperature, which means that activated diffusion is the rate-controlling process. The activation energies E_a (kJ·mol^{-1}) for the adsorption of ethylene and ethane were, respectively, 13.8 ± 1 and 14.6 ± 0.2. The dual Langmuir model described the CO_2 adsorption isotherms, whereas those for C_2H_4 and C_2H_6 were fitted with the Sips model at (293.15 and 323.15) K. Exactly as adsorption capacity, the adsorption

heat profiles behave in accordance with the decreasing order of the polarizability and quadrupole moment of the gas molecules, that is, as follows: $CO_2 > C_2H_4 > C_2H_6$. The equilibrium adsorption selectivity for gas mixtures decreased in the same sequence of decreasing order of quadrupole moment difference ($\delta_1 - \delta_2$) of gases: $CO_2/C_2H_6 > C_2H_4/C_2H_6 > CO_2/C_2H_4$. The obtained results allow the assumption that 4A(CECA) could be a suitable adsorbent for separating CO_2/C_2H_6, C_2H_4/C_2H_6, and CO_2/C_2H_4 mixtures.

Literature Cited

(1) Yang, R. T. *Gas separation by Adsorption Processes*; Butterworth Publishers: Boston, 1987.

(2) Padin, J.; Yang, R. T. New sorbents for olefin/paraffin separations by adsorption via π-compexation; Synthesis and Effects of Substrates. *Chem. Eng. Sci.* **2000**, *55*, 2607–2616.

(3) Chen, L.; Liu, X. π-Complexation Mesoporous Adsorbents Cu-MCM-48 for Ethylene-Ethane Separation. *Chin. J. Chem. Eng.* **2008**, *16*, 570–574.

(4) Al-Baghli, N. A.; Loughlin, K. F. Adsorption of Methane, Ethane, and Ethylene on titanosilicate ETS-10 Zeolite. *J. Chem. Eng. Data* **2005**, *50*, 843–848.

(5) Al-Baghli, N. A.; Loughlin, K. F. Binary and Ternary Adsorption of Methane, Ethane, and Ethylene on Titanosilicate ETS-10 Zeolite. *J. Chem. Eng. Data* **2006**, *51*, 248–254.

(6) Choudhary, V. R.; Mayadevi, S. Adsorption of Methane, Ethane, Ethylene, and Carbon Dioxide on Silicalite-I. *Zeolites* **1996**, *17*, 501–507.

(7) Calleja, G.; Pau, J.; Calles, J. A. Pure and Multicomponent Adsorption Equilibrium of Carbon Dioxide, Ethylene, and Propane on ZSM-5 Zeolites with different Si/Al Ratios. *J. Chem. Eng. Data* **1998**, *43*, 994–1003.

(8) Anson, A.; Wang, Y.; Lin, C. C. H.; Kuznicki, T. M.; Kuznicki, S. M. Adsorption of Ethane and Ethylene on modified ETS-10. *Chem. Eng. Sci.* **2008**, *63*, 4171–4175.

(9) Van Miltenburg, A.; Zhu, W.; Kapteijn, F.; Moulijn, J. A. Adsorptive Separation of Light Olefin Paraffin Mixtures. *Chem. Eng. Res. Des.* **2006**, *84*, 350–354.

(10) Lin, Y. S.; Ji, W.; Wang, Y.; Higgins, R. J. Cuprous-Chloride-Modified Nanoporous Alumina Membranes for Ethylene-Ethane Separation. *Ind. Eng. Chem. Res.* **1999**, *38*, 2292–2298.

(11) Nicholson, T. M.; Bhatia, S. K. Electrostatically Mediated Specific Adsorption of Small Molecules in Metallo-Organic Frameworks. *J. Phys. Chem. B* **2006**, *110*, 24834–24836.

(12) Choudhary, V. R.; Mayadevi, S. Sorption Isotherms of Methane, Ethane, Ethylene, and Carbon Dioxide on ALPO-5 and SAPO-5. *Langmuir* **1996**, *12*, 980–986.

(13) Breck, D. W. *Zeolite Molecular Sieves*; J. Wiley & Sons: New York, 1974.

(14) Timofeev, D. P.; Erashko, I. T. Sorption Kinetics of Water Vapor on Type A Zeolites. *Izv. Akad. Nauk SSSR, Otd. Khim. Nauk* **1961**, *7*, 1192–1197, In Russian.

(15) Dewitt, A. C.; Herwig, K. W.; Lombardo, S. J. Adsorption and Diffusion Behavior of Ethane and Ethylene in Sol-Gel Derived Microporous Silica. *Adsorption* **2005**, *11*, 491–499.

(16) Keltsev, N. V. *Fundamentals of Adsorptive Technique* (In Russian); Khimia: Moscow, 1976.

(17) Duong, D. D. Adsorption Analysis: Equilibria and Kinetics. *Series on Chemical Engineering*, Vol. 2; Imperial College Press: London, 1998.

(18) Reed, T. B.; Breck, D. W. Crystalline Zeolites. II. Crystal Structure of Synthetic Zeolite, Type A. *J. Am. Chem. Soc.* **1956**, *78*, 5972–5977.

(19) Chudasama, D. C.; Sebastian, J.; Jasra, R. V. Pore-Size Engineering of Zeolite A for the Size/Shape Selective Molecular Separation. *Ind. Eng. Chem. Res.* **2005**, *44*, 1780–1786.

(20) Lewis, W. K.; Gilliland, E. R.; Chertow, B.; Cadogan, W. P. Adsorption Equilibria Hydrocarbon Gas Mixtures. *Ind. Eng. Chem.* **1950**, *42*, 1319–1326.

(21) Myers, A. L. Adsorption of Gas Mixtures, A Thermodynamic Approach. *Ind. Eng. Chem.* **1968**, *60*, 45–49.

(22) Newalkar, B. L.; Choudary, N. V.; Turaga, U. T.; Vijayalakshmi, R. P.; Kumar, P.; Komarneni, S.; Bath, T. S. G. Adsorption of Light Hydrocarbons on HMS Type Mesoporous Silica. *Microporous Mesoporous Mater.* **2003**, *65*, 267–276.

(23) Hyun, S. H.; Danner, R. P. Equilibrium Adsorption of Ethane, Ethylene, Isobutane, Carbon dioxide, and Their Binary Mixtures on 13X Molecular Sieves. *J. Chem. Eng. Data* **1982**, *27*, 196–200.

(24) Triebe, R. W.; Tezel, F. H.; Khulbe, K. E. Adsorption of Methane, Ethane and Ethylene on Molecular Sieves Zeolites. *Gas Sep. Purif.* **1996**, *10*, 81–84.

Received for review March 9, 2010. Accepted August 15, 2010. The authors thank the Consejo Nacional de Ciencia y Tecnología (CONACYT, México) for financial support via a scholarship (No. 189933) for Á.R.P.

JE100215C